Journal of Agricultural Engineering

https://www.agroengineering.org/

Intelligent monitoring system for plastic film and drip tape laying quality in film mulching planters based on multi-sensor fusion

Haoqiang Sun,[1,2,3] Jincheng Chen,[1,2] Baiwei Wang,[1,2] Yuze He,[1,2] Chao Ji[1,2]

[1]Mechanical Equipment Research Institute, Xinjiang Academy of Agricultural and Reclamation Science, Shihezi
[2]Key Laboratory of Northwest Agricultural Equipment, Ministry of Agriculture and Rural Affairs, Shihezi
[3]College of Mechanical and Electrical Engineering, Shihezi University, Shihezi, China

Corresponding author: Chao Ji, Mechanical Equipment Research Institute, Xinjiang Academy of Agricultural and Reclamation Sciences, Shihezi 832000, China. E-mail: jicobear@163.com

Please cite this article as doi: 10.4081/jae.2026.2099

Submitted: 14 January 2026
Accepted: 15 April 2026

Intelligent monitoring system for plastic film and drip tape laying quality in film mulching planters based on multi-sensor fusion

Haoqiang Sun,[1,2,3] Jincheng Chen,[1,2] Baiwei Wang,[1,2] Yuze He,[1,2] Chao Ji,[1,2,]

[1]Mechanical Equipment Research Institute, Xinjiang Academy of Agricultural and Reclamation Science, Shihezi
[2]Key Laboratory of Northwest Agricultural Equipment, Ministry of Agriculture and Rural Affairs, Shihezi
[3]College of Mechanical and Electrical Engineering, Shihezi University, Shihezi, China

Corresponding author: Chao Ji, Mechanical Equipment Research Institute, Xinjiang Academy of Agricultural and Reclamation Sciences, Shihezi 832000, China. E-mail: jicobear@163.com

Contributions: All authors read and approved the final version of the manuscript and agreed to be accountable for all aspects of the work.

Conflict of interest: The authors declare that they have no known competing financial interests or personal relationships that could have appeared to influence the work reported in this paper.

Availability of data and materials: All data generated or analyzed during this study are included in this published article.

Acknowledgments: this research was funded by the Young Science and Technology Top Talent Program of Tianshan Talent Training Program of Xinjiang Production and Construction Corps (No. 2022TSYCCX0123), and the Natural Science Research Program of Xinjiang Production and Construction Corps(2025DA039), and the Agricultural Machinery and Equipment Industry Chain Special Fund Project of Xinjiang Production and Construction Corps (No. 2025CYL02).

Abstract

Manual monitoring of plastic film and drip tape laying quality during mulch-covered seed drill operations is limited by high labor intensity, delayed fault detection, and unstable accuracy. To solve these problems, this study proposes a multi-source data acquisition method combining depth cameras and inductive proximity switches, and develops a dedicated monitoring system with a Raspberry Pi 5 as the core controller. Aiming at the key challenges of accurate mulch film segmentation and limited

computing power of edge devices, an enhanced lightweight YOLOv11n-seg-DBM segmentation model is proposed, it integrates a C3k2-DWR module to enhance multi-scale feature extraction, a C2BRA module to optimize cross-layer feature interaction, an MFM module for dynamic feature fusion, and a Focaler-CIoU loss function to improve hard sample mining. After pruning and quantization, the model is successfully deployed on edge devices. The system achieves quantitative detection of mulch exposed area and soil coverage width *via* sub-pixel edge detection and depth information calculation, and realizes real-time fault diagnosis and alarm for film and tape breakage through proximity switch signal sequence analysis. Ablation test results show the improved model outperforms the baseline by 3.52 percentage points in mIoU and 3.35 percentage points in MPA, with parameters reduced to 2.75M Field trials confirm average monitoring accuracies of 93.05% for mulch exposed area and 93.02% for soil coverage width, with average response times of 1.21 s for film breakage and 1.59 s for tape breakage. This study provides an effective technical solution for intelligent operation monitoring and quality improvement of mulch-covered seed drills.

Key words: monitoring system; plastic film and drip tape laying; YOLO11.

Introduction

According to the 2024 China Rural Statistical Yearbook, China's nationwide agricultural plastic mulch usage reached 1.375 million tonnes in 2023, covering 17,764.1 thousand hectares of farmland. The Xinjiang Uygur Autonomous Region, as the core bulk crop production hub in China's arid and semi-arid zones, accounted for 295,000 tonnes of mulch consumption and 3,990.1 thousand hectares of mulched area that same year, leading the country in both metrics. This extensive, concentrated mulch application in Xinjiang imposes strict requirements on the operational quality of mulch-laying seeding equipment, and directly underpins the practical value and urgent application demand for the intelligent monitoring method proposed in this study. During mulch-covered sowing operations, common challenges include film/tape breakage, insufficient light penetration, and difficulty detecting depleted consumables (Sun *et al*., 2016; Su *et al*., 1998). Currently, widely used mulch-laying seed drills operate at speeds of 3-4 km/h (Liao *et al*., 2020; Chen *et al*., 2010; Li *et al*., 2016), yet still rely on manual real-time monitoring of operational quality. This results in high labor intensity and delayed fault detection, subsequently impacting sowing quality,

plastic film light transmission, and temperature-enhancing effects, ultimately reducing crop yields and profitability. Therefore, intelligent upgrades to mulch-laying seed drills are required to achieve real-time, precise monitoring and control of operations, thereby meeting the demands of modern agriculture.

State of the art

Existing research has explored monitoring systems for agricultural film-laying and pipe-laying operations to a limited extent. Bai *et al*. (2025) utilized a disc-type seed drill from Xinjiang as a platform, employing color fiber optics and machine vision technology. They developed a cotton precision film-laying and seed-drilling machine operation quality monitoring system using LabVIEW, verifying the system's stability and practicality. However, this system focuses on monitoring the quality of sowing, but lacks accurate detection of the quality and morphological characteristics of the membrane tubes laid out. Li *et al*. (2024) addressed issues such as film breakage, belt failure, and belt jamming in peanut film-covered seeders by designing a key operational parameter monitoring system, achieving effective fault detection. Nevertheless, current research on monitoring the condition of plastic mulch itself during the laying process remains insufficient.

Most existing studies on agricultural machinery operation quality monitoring focus on sowing link monitoring, while research on the condition monitoring of plastic mulch itself during the laying process remains insufficient. Zhang *et al*. (2022) developed a seed retrieval status monitoring system for cotton precision hole-sowing machines to address the issue of empty holes caused by poor seed retrieval and distribution during cotton precision hole-sowing operations, effectively resolving the challenge of detecting empty holes in cotton sowing. Jia *et al*. (2018) addressed the seed suction mechanism in pneumatic seed feeders during high-speed precision sowing by designing a seed suction status detection system. This system employs a concave photoelectric sensor combined with a photoelectric rotary encoder to monitor the feeder's operational condition. Tan *et al*. (2014) proposed a machine vision and BP neural network-based detection technique for super hybrid rice cell sowing quantities. This ensured consistent super hybrid rice seed numbers per cell on seed trays, enabling precision sowing operations. The system achieved accurate monitoring of cell sowing quantities with an average accuracy rate of 94.4%.These studies provide technical references for agricultural machinery operation monitoring, but cannot be directly

applied to film laying quality monitoring due to the differences in monitoring objects and scenarios.

With advances in artificial intelligence technology, segmentation algorithms based on deep learning have achieved significant progress. Niu *et al*. (2023) addressed the challenge of identifying plastic greenhouses and plastic mulch-covered farmland in VHR remote sensing imagery by proposing an improved semantic segmentation model. This model integrates spectral, textural, and spatial topological features of land cover to enhance recognition accuracy. Ning *et al*. (2021) combined UAV multispectral imagery with convolutional neural networks, incorporating a sub-attention mechanism within the DeepLabv3+ architecture to improve plastic film detection accuracy in complex scenarios.

In recent years, lightweight YOLO segmentation models have been widely used in real-time agricultural vision tasks due to their excellent balance between accuracy and inference efficiency. Jin *et al*. (2026) addressed challenges in rock fissure detection and segmentation -including imbalanced sample distribution, insufficient learning for difficult-to-classify samples, and difficulties in small-object segmentation- by proposing YOLO11n-seg-RF, a lightweight rock fissure detection and segmentation algorithm based on an improved YOLO11n-seg. This model establishes a porosity-compressive strength equation by calculating the proportion of cracks and combining it with uniaxial compression tests, enabling rapid estimation of uniaxial compressive strength. Wu *et al*. (2025) proposed an improved lightweight instance segmentation model, YOLOv8n-seg, for crack detection tasks, achieving 94.5% detection accuracy with excellent real-time performance. Zhang *et al*. (2024) addressed challenges posed by surface stains and occlusions on dairy cows, proposing an enhanced YOLO v8n-seg cow body segmentation algorithm. Under occluded target conditions, this algorithm achieved 93.8% precision with a mean average precision of 93.15%. Despite extensive research on monitoring systems and segmentation algorithms, a notable gap persists in studies directly applying these to quality monitoring of film-laying and pipe-laying operations in mulch-laying seeders.

To fill the above research gaps, this study proposes a multi-sensor fusion monitoring system for film and drip tape laying quality of mulch-laying seed drills. We integrate sensor technology and computer vision technology to realize comprehensive monitoring of film laying dimensional indicators and fault states. Meanwhile, we propose an improved YOLO11n-seg-DBM lightweight segmentation model for film

segmentation, which achieves an excellent balance between segmentation accuracy and edge inference efficiency. The performance of the model and system is verified through systematic experiments and field trials.

Materials and Methods

Selection of monitoring indicators

To ensure the monitoring system is fully aligned with the practical operational requirements of plastic film mulching and drip tape laying, this study establishes a systematic indicator system for operation quality monitoring by integrating formal industry standards and field investigation results. In terms of dimensional quality control for film laying, two core indicators are determined with reference to the quality specifications for plastic film laying in the industry standard JB/T 7732-2023 Plastic Film Laying and Seeding Machines, namely the width of the film light-receiving surface and the width of soil covering at the film edge. The width of the light-receiving surface directly determines the heat preservation and light transmission efficiency of the mulch film, a key parameter affecting the crop growth environment, while the width of soil covering at the film edge is closely related to the laying stability, wind resistance and moisture retention capacity of the mulch film. Both indicators require continuous quantitative monitoring to ensure the film laying effect meets preset agronomic requirements. Field investigations show that mulch-laying seeders frequently suffer from operation failures during field work, mainly including rupture of the mulch film as well as breakage of the drip tape, the latter of which is mostly caused by uneven forward speed of the implement leading to drip tape entanglement in the support frame. Accordingly, two fault monitoring indicators are set for the system, which are real-time detection of mulch film rupture and real-time detection of drip tape breakage.

The establishment of the above indicator system comprehensively considers agronomic requirements, operational stability and fault response requirements, and balances the technical feasibility of the system and its practicability in complex field environments. This ensures the system has strong adaptability and operability in actual production, and lays a solid theoretical foundation for subsequent sensor selection, data acquisition scheme design and intelligent control strategy development. The definition of the two core dimensional indicators is illustrated in Figure 1, which shows the cross-section of film and drip tape laying by the mulch seeder.

Overall design of the monitoring system

The film and drip tape laying quality monitoring system developed in this study adopts a Raspberry Pi 5 as the core controller, integrated with an Intel RealSense D435i depth camera for mulch image and depth data acquisition, E2CE-M30KN30W-C12M inductive proximity switches for film status monitoring, a hollow-shaft encoder for drip tape breakage monitoring, a robotic regulated power supply expansion board, a 13.3-inch Raspberry Pi display module for human-machine interaction, an isolation relay. The system's overall framework is shown in Figure 2, with its workflow consisting of three core stages: data acquisition, data analysis and processing, and feedback alarm.

In operation, the depth camera captures real-time images of the laid plastic mulch, and the improved YOLO11n-seg-DBM model is used for mulch region segmentation. The film's light-receiving surface width and soil covering width are calculated by combining depth information and camera installation parameters.

For film roll monitoring, a metal wire is affixed to the inner side of the film roll core, and the proximity switch detects periodic pulse signals from its rotation; the film is deemed exhausted or broken if no signal is received for more than two complete pulse cycles. For drip tape monitoring, non-metallic markers are fixed on the drip tape reel, and their passage is detected by the proximity switch; the system judges the drip tape as broken or exhausted when no signal is received for more than one full pulse cycle. The system displays real-time operational parameters and mulch images via the human-machine interface, and triggers pop-up alerts immediately upon anomaly detection.

Drip tape is prone to breakage or jamming due to uneven implement speed or reel stalling, which severely impairs operational quality, so a hollow-shaft encoder is adopted for monitoring. During normal laying, the encoder's pulse frequency rises steadily as the reel diameter decreases with tape unwinding. A sudden drop or complete stop of the pulse signal indicates drip tape breakage or jamming, and the system diagnoses the fault immediately. The system displays real-time operational parameters and mulch images on the human-machine interface and triggers instant pop-up alerts upon anomaly detection.

Research on plastic mulch segmentation methods based on the YOLO11 model

Preparation and processing of plastic mulch datasets

Image data of plastic mulch were acquired in the experimental fields of the Xinjiang Academy of Agricultural Sciences using an Intel RealSense D435i camera.

Images were captured under diverse natural lighting conditions, including overcast and clear skies, front-lit and backlit scenes, and different time periods of morning, midday and evening, yielding a total of 1500 raw images. The dataset was randomly split into training, validation, and test sets at an 8:1:1 ratio, and augmented via translation, flipping, noise injection, and brightness adjustment to expand sample size and improve model robustness. All images were annotated with Labele, and the resulting annotation files were converted into a neural network-compatible .txt format for deep learning model training.

YOLO11 segmentation model architecture

The YOLO11 model, developed by Ultralytics, is a unified neural network supporting image classification, object detection, and semantic segmentation. Compared with previous YOLO variants, YOLO11 achieves significant improvements in detection performance and inference speed via architectural optimization, enabling high-accuracy, reliable deployment for real-time applications.

The YOLO11 segmentation model comprises four core modules: Input Layer, Backbone Network, Neck Network and Segmentation Head. The Input Layer processes raw images through preprocessing (resizing, normalization) and integrates Mosaic data augmentation during training to enrich contextual information and enhance model robustness (Wang *et al*., 2023). The Backbone extracts deep features via stacked convolution and pooling operations, generating multi-level semantic feature maps. The Neck adopts a hybrid FPN-PAN architecture to fuse and enhance the Backbone's multi-scale features, aggregating shallow fine-grained localization information and deep high-level semantic information to build a high-resolution, semantically robust feature pyramid for subsequent segmentation and detection tasks. As the core output module, the Segmentation Head is equipped with three branches for 8x, 16x and 32x downsampling scales, realizing accurate multi-scale segmentation and boundary localization of plastic mulch (Wang CY *et al*., 2025; Wang A *et al*., 2024).

To meet the core requirements of real-time performance and computational efficiency for plastic mulch monitoring tasks, this study takes the lightweight YOLO11n-seg model as the baseline, and proposes a series of targeted architectural improvements to enhance the segmentation accuracy and edge detail representation of plastic mulch regions. The optimized model, denoted as YOLO11n-seg-DBM, has its network architecture illustrated in Figure 3. Specifically, in the Backbone, we introduce

the Convolutional 3-Kernel Dilated Residual Feature Enhancement Module (C3k2-DWR) to strengthen multi-scale feature interaction, and reconstruct the original Convolutional 2-Pooling Attention (C2PSA) module with the Bidirectional Routing Attention (BRA) module to further optimize the representation capability of multi-scale features. In the intermediate layer, the original concatenation operation is replaced with the Modulation Fusion Feature Module (MFM), which realizes adaptive feature fusion *via* a dynamic weight modulation mechanism and thus improves the efficiency of information fusion.

Dilation-wise residual module

The original YOLO11n-seg model uses the C3k2 module as the core feature extraction unit, but its multi-scale feature capture capacity for thin plastic mulch is insufficient in complex agricultural environments, leading to poor anti-interference performance. To solve this problem, this paper replaces the C3k2 module in the high-resolution feature layer of the YOLO11n-seg backbone with the proposed C3k2-DWR module, to enhance the model's multi-scale feature representation and high-level receptive field extraction capability for mulch targets. Wei *et al*. (2022) proposed the robust DWRSeg (Dilation-wise Residual Segmentation) network, where the DWR (Dilation-wise Residual) module serves as its core component. Specifically designed for efficient acquisition of multi-scale contextual information, it resolves the inefficiency of traditional dilated convolutions in real-time semantic segmentation through an innovative 'two-step residual feature extraction method.

In terms of comprehensive performance, the DWR module brings three key improvements for mulch segmentation tasks. First, in feature extraction efficiency, the two-step pipeline reduces redundant calculations such as unnecessary receptive field operations on background regions; the convolution and ReLU activation in regional residualization enhance key mulch features and suppress noise, enabling subsequent dilated convolutions to extract morphological information more efficiently with minimal feature confusion. Second, in segmentation accuracy, multi-rate dilated convolutions selectively capture multi-scale contextual information of mulch: small dilation scales refine edge details to reduce boundary blurring and improve localization precision, while large dilation scales strengthen regional semantic perception to accurately distinguish mulch from similar backgrounds, making segmentation results more consistent with the actual mulch morphology. Third, in complex scenario

adaptability, when facing adverse field conditions such as uneven illumination or crop occlusion, the stepwise feature processing of the DWR module first filters partial environmental noise via regional residualization, then adapts to different occlusion patterns via semantic residualization to identify residual mulch regions under obstructions. This significantly enhances the model's robustness to complex scenarios, stabilizes segmentation performance, and mitigates accuracy fluctuations caused by environmental interference.

In summary, the DWR module optimizes the feature extraction process via the two-step residual paradigm, which fully meets the task requirements of mulch segmentation and the lightweight positioning of the baseline model. It is expected to comprehensively improve the efficiency, accuracy and robustness of the YOLO11n-seg model for plastic mulch segmentation, enabling lightweight models to efficiently handle practical field monitoring challenges. The structure of the C3k2-DWR module is shown in Figure 4.

Bi-level routing attention module

In the field mulch segmentation task, there are challenges such as semantic confusion between mulch and soil, incomplete features due to blurred film edges, and precise localization of multi-scale mulch regions in complex backgrounds. To address this, this study introduces the Bi-Level Routing Attention (BRA) module to reconstruct the original C2PSA module, and the improved C2BRA module is obtained. The structure of the C2BRA module is shown in Figure 5.

The BRA module is a component designed to enhance computational efficiency in attention mechanisms (Long *et al*., 2024). It adopts a dynamic query-based sparse attention mechanism to reduce the computational cost and memory footprint of traditional multi-head self-attention. It first partitions the input feature map into S×S non-overlapping regions, and realizes coarse-to-fine attention calculation through a two-stage routing mechanism. The regional affinity matrix is calculated by the following formula:

$$A^r = Q^r \cdot (K^r)^T \quad \text{(Eq. 1)}$$

Where T is the transpose of the matrix; A^r denotes the regional affinity matrix，representing the correlation degree between different regional feature vectors; Q^r denotes the regional query feature matrix, extracted from the regional feature map of plastic mulch images; K^r denotes the regional key feature matrix，mapped from the

regional feature map of plastic mulch images； superscript r is the identifier of regional feature level, distinguishing the feature matrix at the regional segmentation stage from the pixel-level feature matrix. The routing index I^r is obtained through screening to realize coarse-grained regional correlation screening; the "gather" operation is performed on the original key values according to I^r to obtain the gathered K^{gather} and V^{gather}. The attention weight is calculated by the matrix multiplication of Q and K^{gather}, and the output O is generated by weighted summation with V^{gather}.

The dual-layer routing attention mechanism in the C2BRA module first rapidly filters out irrelevant backgrounds like large soil areas through regional-level screening, then performs detailed calculations on challenging regions such as plastic mulch edges. This enhances feature weights in key areas while reducing background interference, and avoids redundant computations on irrelevant regions, which significantly improves the model's feature extraction efficiency in high-resolution mulch images.

Modulation fusion feature module

In complex field environments, background noise such as dust and soil particles easily interferes with the edge features of the plastic film, degrading edge discrimination. To address this issue, this study replaces the traditional concatenation operation in the neck network with the Modulation Fusion Feature (MFM) module, to realize adaptive feature fusion based on feature importance. The structure of the MFM module is shown in Figure 6.

The MFM module first receives local and convolved features, uses Global Average Pooling (GAP) to capture global information, and enables the model to grasp the overall feature context of the mulch distribution. Subsequently, a Multi-Layer Perceptron (MLP) and Softmax function are used to generate a weight matrix that assigns importance to different features, emphasizing mulch-related elements while suppressing noise. Finally, features are fused according to these weights before being passed to subsequent modules.

Compared with the traditional fixed-weight concatenation operation, the MFM module realizes selective enhancement of useful information, which makes the key characteristics of plastic mulch more prominent, suppresses interference from dust and complex backgrounds, and improves the model's segmentation accuracy for mulch edges and small fragments.

Loss function focaler-CIoU

For bounding box regression, the CIoU loss function is widely adopted in the YOLO series, which simultaneously accounts for the overlap area, position offset, and aspect ratio consistency between the predicted box and ground-truth box (Zheng *et al*., 2020). However, sample imbalance is a prevalent challenge in object detection and segmentation tasks: samples can be categorized into hard and easy samples according to learning difficulty, while traditional loss functions assign equal weights to all samples. This causes the model to be dominated by abundant easy samples during training, and neglects feature learning from critical hard samples. To address the insufficient bounding box regression accuracy in segmentation tasks, this paper adopts the improved Focaler-CIoU loss function. Its core innovation lies in integrating the geometric constraint capability of CIoU with the hard-sample focusing property of the focal mechanism, and realizing differentiated optimization for samples of varying difficulty via dynamic weight assignment. The calculation formula is as follows:

$$IoU_{map} = (\frac{IoU-d}{u-d})_{clamp(0,1)} \quad \text{(Eq. 2)}$$

$$\upsilon = \frac{4}{\pi^2}(arctan\frac{w_2}{h_2} - arctan\frac{w_1}{h_1})^2 \quad \text{(Eq. 3)}$$

$$\alpha = \frac{\upsilon}{(1-IoU_{map})+\upsilon} \quad \text{(Eq. 4)}$$

$$CIoU = IoU_{map} - (\frac{\rho^2}{c^2} + \alpha\upsilon) \quad \text{(Eq. 5)}$$

$$L_{Focaler-CIoU} = -\alpha_t(1 - CIoU)^{\gamma}\log(CIoU) \quad \text{(Eq. 6)}$$

Where d is the lower limit preset threshold of IoU, u is the lower limit preset threshold of IoU, and the mapping result is constrained to the [0,1] interval through the clamp (0,1) operation to avoid the dominance of extreme values on the loss; ρ is the distance between the centers of the predicted box and the real box; c is the diagonal distance of the minimum box of the predicted box and the real box; υ is a parameter measuring the consistency of the aspect ratio; α is a weight function; IoU is the ratio of the intersection and union of the real box and the predicted box; α_t is used to balance the proportion of positive and negative samples, and γ is a focusing parameter, which makes the loss function assign higher weight to hard samples with low CIoU and lower attention to easy samples with high CIoU, realizing differentiated learning.

The core of the Focaler-CIoU loss function is to reconstruct the original Intersection over Union (IoU) via linear interval mapping, to achieve targeted

optimization for regression samples with different difficulty levels. Unlike the traditional CIoU loss, which introduces center distance and aspect ratio consistency constraints based on IoU but applies equal weight to all samples, Focaler-CIoU introduces adjustable hyperparameters to assign sample-wise dynamic weights according to the IoU gap between predictions and ground truths, thus granting higher training priority to hard-to-segment samples.

This design retains CIoU's precise geometric constraints on bounding boxes, while dynamically adjusting training focus based on sample difficulty: for low-IoU samples (i.e., large deviations between predicted and ground-truth boxes), the loss weight is amplified to force the model to focus on learning these hard samples; for high-IoU samples with relatively accurate predictions, the loss weight is reduced accordingly to avoid overfitting to these easy samples. For samples with medium IoU, the loss weight decreases linearly with increasing IoU, realizing a smooth transition of training weights across samples of different difficulty and mitigating training bias caused by extreme weight assignment.

This loss function is designed to improve the stability and accuracy of model bounding box regression in complex scenarios, providing a more reliable and efficient optimization scheme for fine-grained segmentation tasks.

Training and inference configuration

The development platform for model training and testing in this study is configured with an Intel(R) Core(TM) i7-14700HX @ 2.10 GHz processor, an NVIDIA GeForce RTX 4070 Laptop GPU, and a 64-bit Windows 11 operating system. All models were implemented on the PyTorch framework, with the experimental environment set to Python 3.8.20, torch 1.11.0 and CUDA 11.3. Mosaic data augmentation was applied to all YOLO-series networks during training to improve model generalization. The final training hyperparameters were determined as follows: 200 epochs, batch size of 16, SGD optimizer with an initial learning rate of 0.01, cosine annealing learning rate schedule, momentum of 0.937, and weight decay coefficient of 0.0005.

YOLO model evaluation metrics

Among the performance evaluation metrics commonly used in the field of Image Semantic Segmentation (ISS) as referenced in (Tian *et al*., 2019; Yi *et al*., 2022; Hayat *et al*., 2020; Ma *et al*., 2025; Chen *et al*., 2024; He *et al*., 2025; Song *et al*., 2022; Zhang

et al., 2025), this study ultimately adopts Pixel Accuracy (PA), mean Intersection over Union (mIoU), Parameters, and Recall as the evaluation metrics for network segmentation performance.

Parameters represent the total number of trainable variables in a model. Parameters reflect the model's complexity and storage requirements. PA measures the accuracy of a model's predictions across all pixels, i.e., the proportion of correctly predicted pixels relative to the total number of pixels. Intersection over Union (IoU) quantifies the overlap between predicted segmentation results and ground truth segmentation

$$PA = \frac{TP+TN}{TP+TN+FP+FN} \quad \text{(Eq. 7)}$$

$$IoU = \frac{TP}{TP+FP+FN} \quad \text{(Eq. 8)}$$

$$mIoU = \frac{1}{N}\sum_{i=1}^{N} IoU_i \quad \text{(Eq. 9)}$$

$$Params \sim O\left(\sum_{a=1}^{n} M_a^2 \cdot K_a^2 \cdot C_{a-1} \cdot C_a\right) \quad \text{(Eq. 10)}$$

Where *TP* is the number of pixels correctly predicted as the target category; *TN* is the number of pixels correctly predicted as the non-target category; *FP* is the number of pixels predicting the non-target category as the target category; *FN* is the number of pixels predicting the target category as the non-target category; *N* is the total number of categories; IoU_i is the IoU of the i-th category; *K* is the convolution kernel size, *C* is the number of channels, *M* is the input image size, and *a* is the number of iterations.

Monitoring system software development

To enable real-time monitoring of membrane and pipe laying operations, the improved YOLO11-seg-DBM segmentation model was deployed on a Raspberry Pi 5. Addressing computational constraints on edge devices, efficient inference was achieved through model pruning and quantization optimization: During pruning, redundant convolutional kernels were removed based on L1 regularization criteria, eliminating channels and layers with contributions below 0.01. The quantization stage employs symmetric INT8 quantization, converting weights and activation values from 32-bit floating-point to 8-bit integers, significantly boosting inference speed. The optimized model was deployed *via* the NCNN framework, leveraging its ARM-architecture-specific instruction set optimizations to further adapt to the Raspberry Pi 5's 64-bit quad-core Cortex-A76 processor. Following mask optimization, sub-pixel edge detection, and depth data computation, the model outputs the exposed area of plastic mulch and soil coverage width. It simultaneously identifies broken film or tape faults

by detecting high/low level signals from proximity switches. The interactive software, developed using PyQt5, displays real-time operational parameters and triggers red pop-up alerts during faults. The system integrates a clear and intuitive visual interface that presents images and monitoring data with precision. It supports multiple file formats for input, ensuring smooth and efficient workflow. Inspection results and logs are saved rapidly and accurately while responding to user commands, completing processing within the specified inspection timeframe. This enables real-time monitoring of film laying and pipe installation, with the overall design process illustrated in Figure 7.

For film segmentation and width calculation, the YOLO11n-seg-DBM model is used for accurate segmentation of the film region, and morphological operations are performed on the segmentation mask output by the model to optimize the segmentation mask through methods such as closing operations. The compensated mask is scanned line by line along the vertical direction of the image, and the pixel coordinates (u_{left},v) and (u_{right},v) of the left and right edges of the film are determined through threshold segmentation. Sub-pixel edge detection is used to improve the positioning accuracy to 0.1 pixel level. According to the mask range of this line, the depth value $Z(v,u)$ of the corresponding region is extracted from the compensated depth image. The abnormal value is removed according to the Laida criterion, and the average value of the effective depth value is calculated to obtain the average depth value $\overline{Zv}$ of this line. The physical width W_v of the film in this line is calculated according to the camera internal parameters and geometric mapping relationship. Accurate calculation of the unilateral soil covering width at the mulch edge is achieved based on central axis segmentation of the plastic mulch and unilateral edge localization, in conjunction with the pre-established camera calibration and depth calculation framework. According to the annotation of the dataset and the training of the model, the film is divided into 5 horizontal sub-regions, and the width of the film is the sum of the widths of the 5 sub-regions. The calculation formulas are as follows:

$$\overline{Z_v} = \frac{1}{N}\sum Z(v,u) \quad \text{(Eq. 11)}$$

$$W_v = \frac{(u_{right}-u_{left})\cdot\overline{Z_v}}{f_x} \quad \text{(Eq. 12)}$$

$$W_{all} = W_{v1} + W_{v2} + W_{v3} + W_{v4} + W_{v5} \quad \text{(Eq. 13)}$$

Where f_x is the horizontal focal length; W_{all} is the width of the film; W_{v1}, W_{v2}, W_{v3}, W_{v4}, W_{v5} are the widths of the 5 sub-regions respectively.

Display module

In the quality monitoring system for film laying and pipe laying operations on film-laying seeders, the human-machine interface serves as a vital bridge between operators and equipment. As shown in Figure 8, this interface features a concise and intuitive layout that integrates real-time monitoring data, plastic film imagery display, and control functions. It aims to provide users with an efficient and convenient monitoring and control experience, assisting operators in promptly grasping equipment operational status and film laying quality.

The real-time data display area centrally presents key parameters during operation, enabling users to intuitively grasp relevant data on film laying and pipe placement during the mulch seeder's working process. This facilitates rapid identification of anomalies and timely intervention. The mulch film image display area provides real-time visual information on field film laying conditions. Through these images, operators can visually inspect the film's appearance -including any damage- offering a visual basis for assessing laying quality. The integration of imagery and real-time data ensures comprehensive monitoring of operational quality from both quantitative and qualitative perspectives. The control operation area features “Start”, “Pause” and “Exit” function buttons. The “Start” button initiates the operation monitoring and equipment operation process, placing the system into data collection, image acquisition, and operation quality monitoring mode. The ‘Pause’ button allows users to temporarily interrupt operations when needed, facilitating equipment debugging or addressing field anomalies. During pauses, the system retains current status data, and operations resume upon pressing “Start” The “Exit” button shuts down the monitoring system, concluding the operation monitoring process, ensuring operational convenience and flexibility.

Field trial design

To evaluate the stability and monitoring accuracy of the proposed monitoring system under actual field operation conditions, field trials were conducted at the experimental fields of the Xinjiang Academy of Agricultural Sciences. The test day featured clear weather with no precipitation and minimal dust, which is fully consistent with the actual operation environment of mulch-covered seed drills in agricultural production.

The experimental equipment used in the field trial includes a Lovol Euro Leopard M904-D tractor with a rated power of 90 hp, a 2MBJ-1/6 mulch-laying seeder matched

with the tractor that integrates 6-row sowing and mulch laying functions, and the mulch and drip tape laying quality monitoring system proposed in this study. The monitoring system consists of a Raspberry Pi 5 main control unit, an Intel RealSense D435i depth camera, inductive proximity switches, a human-computer interaction touch screen, and a supporting power supply module, and the overall layout of the field trial setup is shown in Figure 9.

Before the formal test, the monitoring system was installed and debugged on the mulch-laying seeder, followed by system power-on, historical data clearing, and calibration of the depth camera and proximity switches, to ensure the accuracy of data collection of each functional unit. After the pre-test preparation was completed, the tractor was started to drive the mulch-laying seeder to advance at a constant speed of 3 km/h, which is the common operation speed of mulch-covered seed drills in actual agricultural production, to ensure that the test conditions are consistent with the actual field operation scenarios.

The formal test was carried out in four randomly selected sub-plots in the test area, with two alternating one-way operation paths set in each sub-plot. At 30 randomly selected time points across the four sub-plots, the system automatically collected and recorded the real-time data of the mulch light-transmitting surface width and the soil coverage width on both sides of the mulch edges. Meanwhile, manual measurement of the corresponding indicators was carried out using a tape measure at the same time points, and the manual measurement values were taken as the ground truth to calculate the monitoring accuracy of the system.

To test the fault response performance of the system, the fault monitoring success rate and average response time were adopted as the core validation indicators, where the response time is defined as the time interval between the actual occurrence of plastic film or drip tape breakage and the moment when the system triggers the alarm signal. The field test was carried out in the experimental fields of the Xinjiang Academy of Agricultural and Reclamation Science, with irrigated sandy loam as the soil type, and the field surface was rotary-tilled and leveled prior to the test. The operating speed of the implement was set at a constant 3 km/h during the test. To simulate sudden breakage faults of plastic film and drip tape, 20 pre-cut segments of plastic film and 20 pre-cut segments of drip tape were wound onto the film reel and drip tape reel respectively, and corresponding fault monitoring tests were conducted separately for each fault type.

Results and Discussion

YOLO11n-seg-DBM segmentation model performance evaluation

This study comprehensively evaluates the effectiveness, generalization capability, and performance advantages of the YOLO11n-seg-DBM algorithm in plastic mulch image segmentation tasks through systematic ablation experiments and comparative tests against multiple mainstream segmentation models.

Dissolution test

To validate the effectiveness of each module in the improved YOLO11n-seg-DBM segmentation model, ablation tests were conducted using the YOLO11n model as the baseline model under identical training environments and hyperparameter settings. The results are shown in Table 1.

In terms of the individual performance of each module, the standalone introduction of the C3k2-DWR module increased the model's mean Intersection over Union (mIoU) from the baseline 88.10% to 89.54%, a rise of 1.44 percentage points, with Pixel Accuracy (PA) improved by 0.74 percentage points. These results demonstrate that the C3k2-DWR module effectively enhances the model's feature extraction capability, enabling accurate capture of target features and thus improving the model's semantic segmentation accuracy. The standalone C2BRA module yielded a limited improvement in segmentation performance, with only a 0.50 percentage point increase in mIoU and nearly unchanged number of parameters. When the MFM module was introduced alone, mIoU increased by 0.89 percentage points and PA rose by 1.20 percentage points, with negligible fluctuation in parameters, indicating that the MFM module enables finer-grained feature analysis and thus boosts overall model performance.

For the combined effect of multiple modules, the integration of C3k2-DWR and C2BRA showed a significant synergistic effect, achieving an mIoU of 89.65% and reducing the number of parameters to 2.82 M. This confirms that the two modules achieve complementary feature enhancement: although the C2BRA module has limited standalone effect, it processes features from multiple dimensions when paired with C3k2-DWR, optimizing the feature extraction pipeline to improve accuracy while reducing storage overhead. With the further addition of the MFM module, the model performance was substantially improved, with mIoU reaching 90.81% and parameters reduced to 2.75 M. This result verifies the critical role of the MFM module in multi-module collaboration: its multi-scale feature fusion capability efficiently integrates

feature outputs from different modules, greatly improving the model's target recognition and segmentation performance in complex scenarios, while reducing computational cost and optimizing inference efficiency. The final model with all four modules integrated achieved an mIoU of 91.62% and a 3.35 percentage point increase in PA, with fewer parameters than the baseline model. This indicates that although the Focaler-CIoU loss function has a limited standalone effect, it can deeply optimize the loss calculation process when working synergistically with the other three modules, and further improve model accuracy by precisely guiding the model's training direction.

Comparative testing of different partitioning models

To further verify the performance advantages of the YOLO11n-seg-DBM model, this study compared it with current mainstream instance segmentation models on the self-built mulch dataset, including U-Net, DeepLabV3+, Mask-RCNN, YOLOv5n-seg, and YOLOv8n-seg. The comparative test results are shown in Table 2. It can be seen from Table 2 that the YOLO11n-seg-DBM model achieves the best performance in all four core metrics, and has the least number of parameters. Compared with the heavyweight models such as U-Net, DeepLabV3+, and Mask-RCNN, the proposed model has obvious advantages in both segmentation accuracy and model lightweight. Compared with other lightweight YOLO series models, the proposed model still maintains significant performance advantages.

To visually demonstrate the segmentation performance of each model, the results of different models processing plastic film images are visualized, as shown in Figure 10. The Unet and DeepLabV3+ models exhibit noticeable blurring of plastic film boundaries and local segmentation omissions; Mask-RCNN maintained relatively complete plastic film regions but exhibited excessive smoothing at edge details; YOLOv5n-seg and YOLOv8n-seg models showed significant segmentation improvements, though minor discontinuities persisted at the soil-film interface. In contrast, the YOLO11n-seg-DBM model not only accurately identifies the main plastic film area but also effectively captures subtle edge features. It produces more continuous and clear segmentation contours, significantly reducing instances of misclassification and missed segmentation.

Field trial monitoring system performance results

Laying quality monitoring accuracy results

The monitoring accuracy results of the system for mulch light-transmitting surface width and soil coverage width are shown in Table 3.

As shown in Figures 11 and Table 3, compared with manual measurement, the film-laying and pipe-laying operation quality monitoring system designed in this study achieved an average accuracy rate of 93.05% and an average relative error of 7.15% for monitoring the width of the light-receiving surface of the plastic film. The average accuracy rate for monitoring the width of soil covering the film edges was 93.02%, with an average relative error of 7.35%. Analysis indicates that errors stem from factors affecting image segmentation and width calculations during image acquisition and segmentation, including soil, impurities, natural light intensity, and machine vibration, which consequently impact the monitoring system's precision.

Fault response performance results

The fault response performance test results of the system are shown in Table 4. Field test results demonstrate that the system exhibits excellent identification performance and rapid response capability for both plastic film breakage and drip tape breakage faults. Specifically, the system achieves 100% alarm accuracy for drip tape breakage, with an average response time of 1.59 s; for film breakage, it reaches 95% alarm accuracy with an average response time of 1.21 s, with only one false alarm recorded across 20 repeated tests. The single false alarm was caused by disturbance from field operating conditions. During the test, the implement traveled over uneven ground, and severe vibration during film-laying operation led to offset of the plastic film roll. This made the detection distance between the metal marker on the film roll end face and the inductive proximity switch exceed the sensor’s rated detection threshold, so the sensor failed to stably capture the pulse signal of the film roll rotation, thus triggering the false alarm. Overall, the system has high fault identification accuracy and fast response speed. It can trigger an alarm immediately after a fault occurs to remind the driver to stop and adjust the implement in a timely manner, which solves the problems of delayed fault identification and untimely response in traditional manual monitoring. The system can fully meet the requirements of real-time fault monitoring and rapid early warning for film mulching planters in actual field operations.

Conclusions

This study tackles the core problems of high labor intensity and poor intelligence in manual monitoring of film and drip tape laying operations for film mulching planters. By integrating sensor technology with computer vision, a dedicated quality monitoring system for film and drip tape laying was developed. The key research work and main conclusions are summarized as follows:

(1) A multi-sensor fusion quality monitoring system for film and drip tape laying was designed and deployed, with a Raspberry Pi 5 as the core control unit. The system integrates a depth camera and inductive proximity switches to construct a multi-source data acquisition hardware platform, and a human-machine interface was developed based on PyQt5. This interface enables integrated real-time monitoring and instant alarm for the light-transmitting surface width of plastic mulch, soil covering width at mulch edges, and film/tape breakage status.

(2) To address the challenges of accurate plastic mulch segmentation and the computational constraints of edge devices, an improved lightweight segmentation model (YOLO11n-seg-DBM) was proposed based on the YOLO11n-seg baseline. The model is optimized by incorporating the C3k2-DWR, C2BRA and MFM modules, as well as the Focaler-CIoU loss function. It achieves an mIoU of 0.9162 and an MPA of 0.9626, representing a 3.52 percentage point increase in mIoU and a 3.35 percentage point rise in MPA compared with the baseline model, while its parameter size is reduced to 2.75 M. The model strikes an excellent balance among segmentation accuracy, lightweight design and real-time inference performance. In comparison with mainstream segmentation models, it outperforms all counterparts in three core metrics with the least number of parameters, making it highly suitable for edge computing deployment.

(3) Field trials were conducted at the experimental farm of the Xinjiang Academy of Agricultural Sciences to verify the system's performance. The results show that the system achieves an average monitoring accuracy of 93.05% for the light-transmitting surface width of plastic mulch, and 93.02% for the soil covering width at mulch edges. For film and tape breakage monitoring, the system delivers rapid response and reliable identification, with average response times of 1.21 s and 1.59 s, respectively, and maintains low false and missing alarm rates. Overall, the developed monitoring system enables accurate geometric dimension measurement of plastic mulch, fast and precise fault identification of film/tape breakage, and accurate quantification of the longitudinal

elongation rate of drip tape. It exhibits strong adaptability to complex field operating environments and fully meets the practical quality monitoring requirements of film mulching planters in field operations.

While this study delivers valid and promising results for the intelligent monitoring of plastic film and drip tape laying quality, a notable limitation exists regarding the generalizability of the proposed monitoring system. The field trials were exclusively conducted in the experimental farm of the Xinjiang Academy of Agricultural and Reclamation Science with irrigated sandy loam soil, and the system's performance has not been verified in other soil types or different climatic regions of China. This may restrict the direct application of the system in diverse agricultural planting scenarios across the country, and further validation is required for broader promotion.

For future research, multi-site field trials will be carried out in different agricultural regions of China with various soil types and climatic conditions to verify the system's adaptability, and targeted optimizations will be made to the model and hardware according to regional characteristics to enhance its generalizability for large-scale application. In addition, the current research focuses on the quality monitoring of plastic film and drip tape laying only, without covering the simultaneous compound operation links of the film mulching planter such as sowing and fertilization. The monitoring system can be further deeply integrated with the quality monitoring modules of supporting operation links including sowing precision and fertilization uniformity to build a full-process collaborative operation quality monitoring platform for film mulching and sowing, thus realizing the comprehensive quality monitoring of the entire film mulching planting process.

References

Bai SH, Yuan YW, Niu K, Zhou L, Zhao B, Yu Y, 2025. [Design and experiment of operation quality monitoring system for cotton precision film mulching hole seeder].[Article in Chinese with English abstract]. Nongye Jixie Xuebao/Trans Chin Soc Agric Mach 5:49-58.

Chen JC, Ji C, Zhang J, Feng , Li Y, Ma B, 2024. A method for multi-target segmentation of bud-stage apple trees based on improved YOLOv8. Comput Electron Agric 220:108876.

Chen XG, Zhao Y 2010. Development of precision seeder for double plastic film mulching of cotton. T CSAE 26:106-112.

Hayat MA, Wu J, Cao Y. 2020. Unsupervised Bayesian learning for rice panicle segmentation with UAV images. Plant Methods 16:18.

He LH, Zhou YZ, Zhang C, 2025. Application of deep learning-based object segmentation in intelligent rock recognition. Bull Mineral Petrol Geochem 44:525-

541.
Jia H, Lu Y, Qi J, Zhe Z, Liu H, Li Y, Luo X, 2018. [Detection of seed adsorption performance of pneumatic seed metering device by photoelectric sensor combined with rotary encoder].[Article in Chinese with English abstract].T CSAE 34:28-39.
Jin Z, Li H, Yin H, Yang G, Chen Y, Li X, Xai S, 2026. [YOLO11n-seg-RF: an improved lightweight rock fracture detection and segmentation algorithm].[Article in Chinese with English abstract]. Acta Sci Nat Univ Pekin 62:237-252.
Li C, Qin P, Lu D, 2024. Research on monitoring system of peanut film mulching seeder based on single-chip microcomputer. Mod Electron Tech 47:162-170.
Li M, Wang W, Du S, 2016. [Experimental study on adsorption accuracy of pneumatic cotton hole seeder. [Article in Chinese with English abstract]. J Chin Agric Mech 37:10-13.
Liao QX, Wang D, Yao L, 2020. [Design and experiment of punching device of film mulching hole-sowing machine for rapeseed].[Article in Chinese with English abstract]. Nongye Jixie Xuebao/Trans Chin Soc Agric Mach 51:62-72.
Long NHB, Zhang C, Shi Y, Hirakawa T, Yamashita T, Matsui T, Fujiyoshi H, 2024. DeBiFormer: vision transformer with deformable agent bi-level routing attention. arXiv:2410.08582v1
Ma BJ, Wu ZH, Ge Y, Chen B, Zhang H, Xia H, Wang D, 2025. A recognition method for marigold picking points based on the lightweight SCS-YOLO-Seg model. Sensors (Basel) 25:4820.
Ning J, Ni J, He Y, Li L, Zhao Z, Zhang Z, 2021. [Identification of plastic film mulched farmland in UAV multispectral remote sensing image based on convolutional attention].[Article in Chinese with English abstract]. Nongye Jixie Xuebao/Trans Chin Soc Agric Mach 52:213-220.
Niu B, Feng Q, Su S, Yang Z, Zhang S, Liu S, et al. 2023. Semantic segmentation for plastic-covered greenhouses and plastic-mulched farmlands from VHR imagery. Int J Digit Earth 16:4553-4572.
Song Y, Yang D, Xu L, Liu Z, 2022. [Segmenting field rice panicle images using DBSE-Net].[Article in Chinese with English abstract]. T CSAE 38:202-209.
Su H, 1998. Common quality problems and solutions in mechanical film mulching operation. Farm Machin 9.
Sun J, 2016. Research on mechanized technology of plastic film mulching. Agric Sci Technol Equip 3:51-53.
Tan S, Ma X, Wu L, li Z, Liang Z, 2014. [Estimation on hole seeding quantity of super hybrid rice based on machine vision and BP neural network].[Article in Chinese with English abstract]. T CSAE 30:201-208.
Tian X, Wang L, Ding Q, 2019. Survey of image semantic segmentation methods based on deep learning. J Softw 30:440-468.
Wang A, Chen H, Liu L, Chen K, Lin Z, Han J, Ding G, 2024. YOLOv10: real-time end-to-end object detection. arXiv:2405.14458.
Wang CY, Bochkovskiy A, Liao HYM, 2023. YOLOv7: trainable bag-of-freebies sets new state-of-the-art for real-time object detectors. Proc. IEEE/CVF Conference on Computer Vision and Pattern Recognition (CVPR), Vancouver; pp. 7464-7475.
Wang CY, Yeh IH, Liao HYM, 2025. YOLOv9: learning what you want to learn using programmable gradient information. Proc. 18th Eur. Conf. Computer Vision, Milan; pp. 1-21.
Wei H, Liu X, Xu S, Dai Z, Dai Y, Xu X, 2022. DWRSeg: rethinking efficient acquisition of multi-scale contextual information for real-time semantic segmentation. arXiv 2212.01173.

Wu Y, Han Q, Jin Q, Zhang Y, 2023. LCA-YOLOv8-Seg: an improved lightweight YOLOv8-Seg for real-time pixel-level crack detection of dams and bridges. Appl Sci 13:10583.

Yi X, Peng C, Zhang Z, Xiao L, 2022. The defect detection for X-ray images based on a new lightweight semantic segmentation network. Math Biosci Eng 19:4178-4195.

Zhang SJ, Xu XS, Deng HX, 2024. [Cow body segmentation method based on YOLOv8n-seg-FCA-BiFPN].[Article in Chinese with English abstract]. Nongye Jixie Xuebao/Trans Chin Soc Agric Mach 55:282-289.

Zhang X, Zhang H, Shi Z, Jin W, Chen Y, Yu Y, 2022. Design and experiment of monitoring system for seed picking status of cotton precision hole seeder].[Article in Chinese with English abstract]. Nongye Jixie Xuebao/Trans Chin Soc Agric Mach 38:9-19.

Zhang Z, Li C, Wang K, 2025. Lightweight fabric defect segmentation algorithm based on SAC-YOLO. J Xi'an Polytech Univ 39: 9-69.

Zheng Z, Wang P, Ren D, Liu W, Ye R, Hu Q, Zuo W, 2020. Enhancing geometric factors in model learning and inference for object detection and instance segmentation. arXiv: 2005.03572.

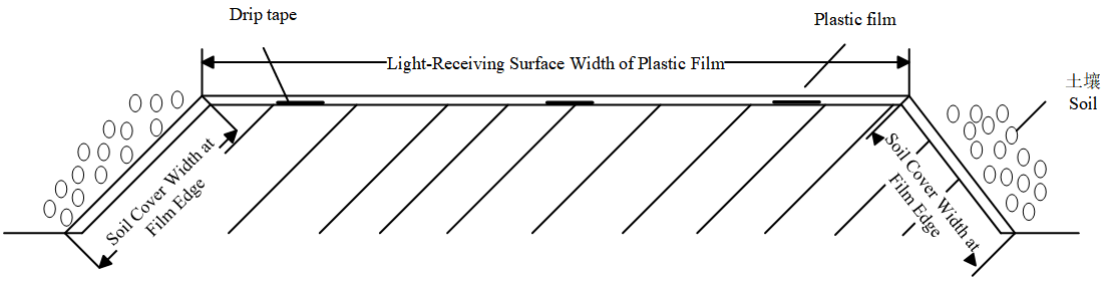

Figure 1. Schematic diagram of the cross-section for film and drip tape laying by a plastic film seeder.

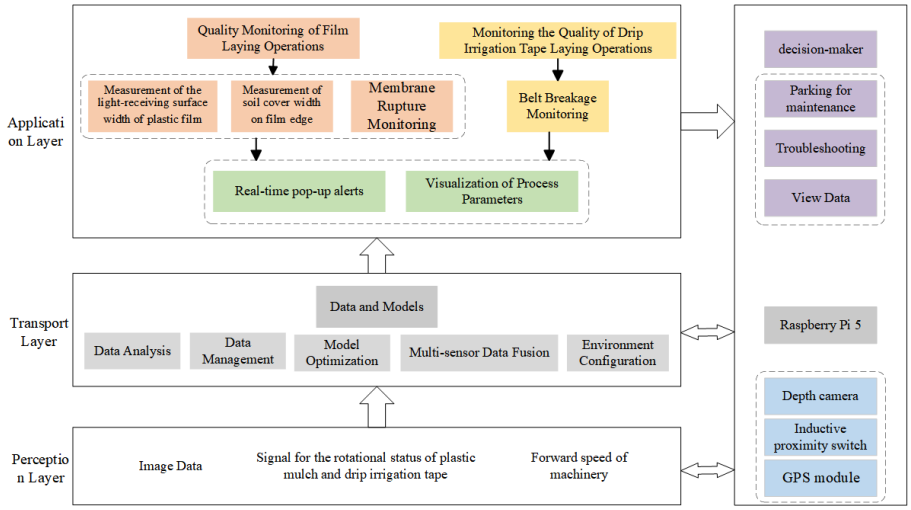

Figure 2. Framework diagram of the quality monitoring system for film and drip tape laying.

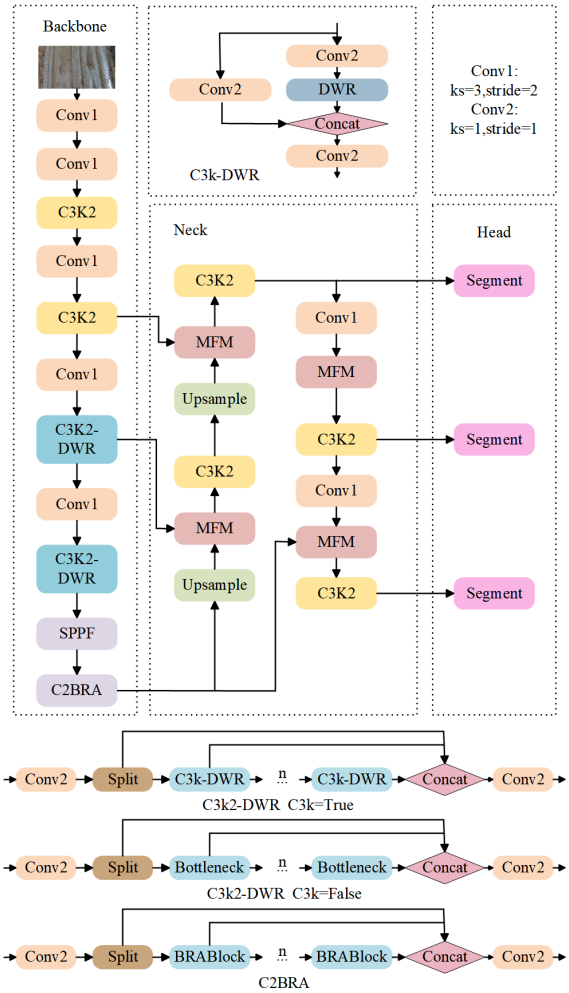

Figure 3. Overall architecture of the YOLO11n-seg-DBM model.

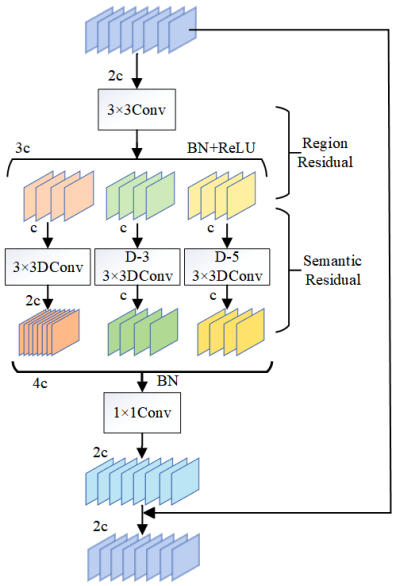

Figure 4. Structure of the DWR module.

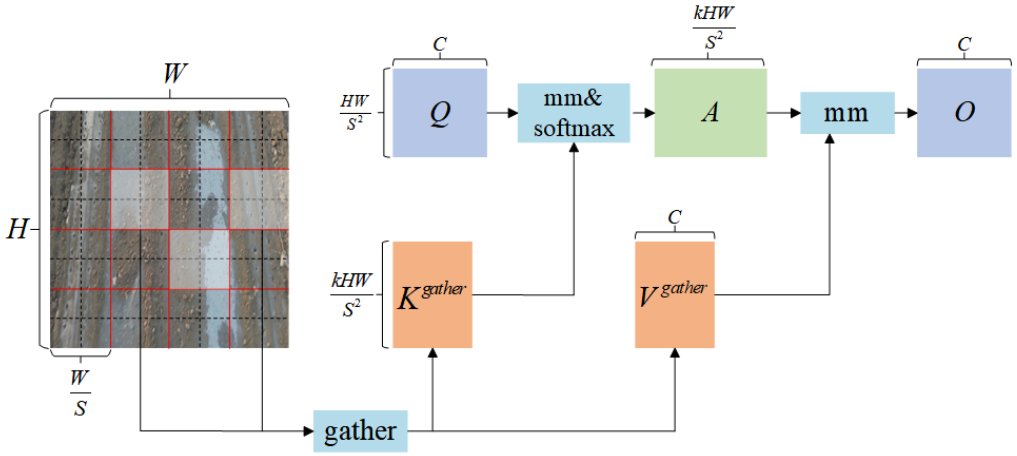

Figure 5. Structure of the BRA module.

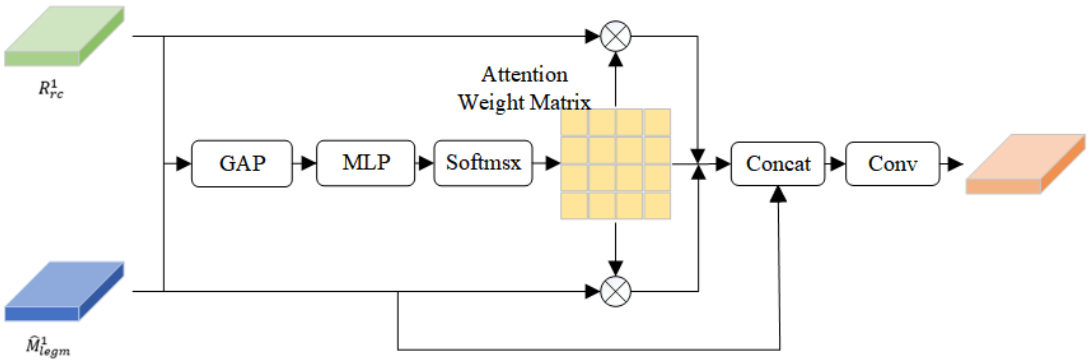

Figure 6. Structure of the MFM module.

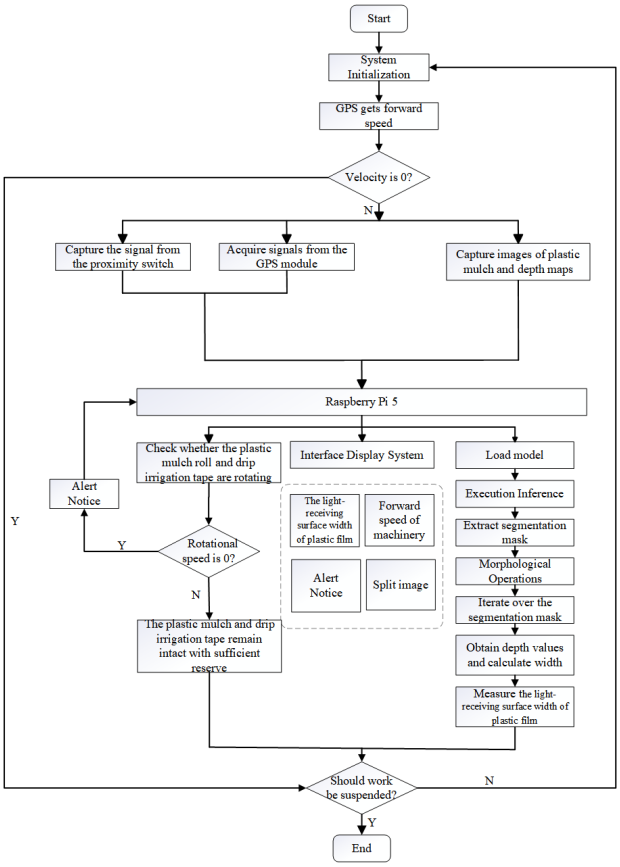

Figure 7. Flowchart of the monitoring system design.

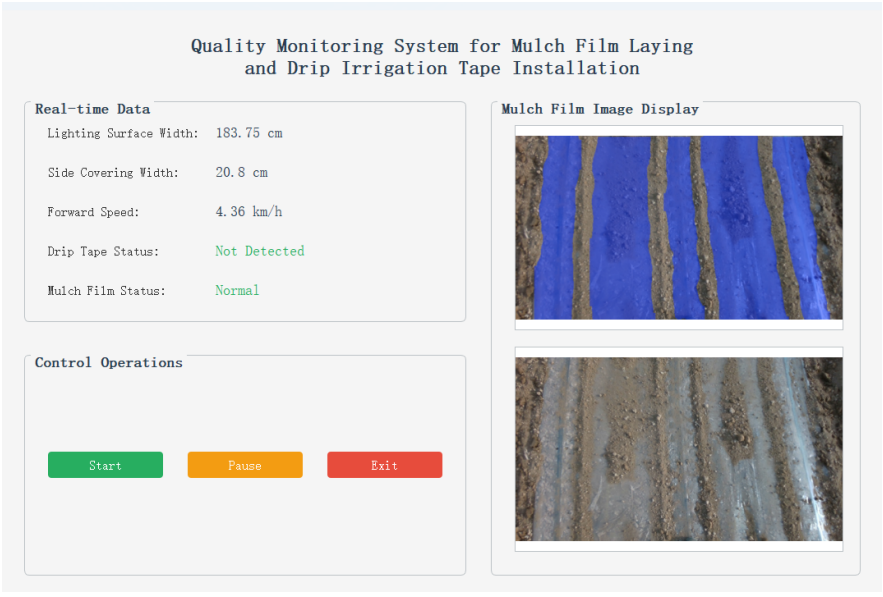

Figure 8. System display interface.

Figure 9. Field experiment.

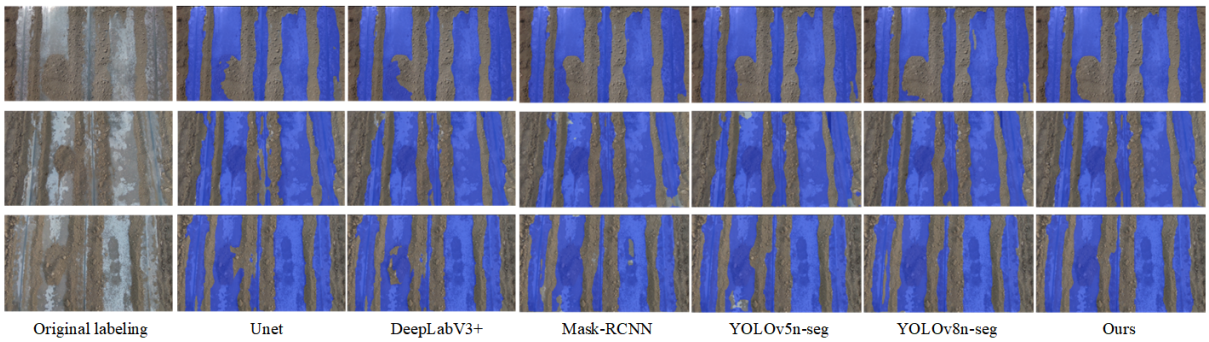

Figure 10. Examples of segmentation effects from different models.

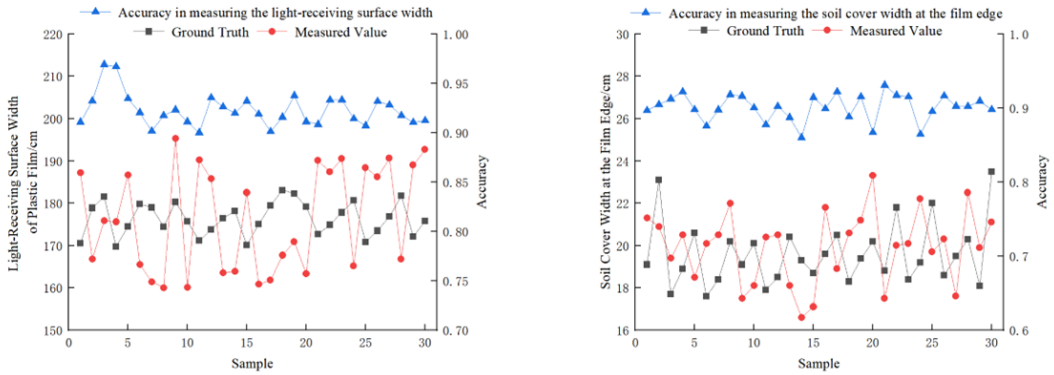

a. Light-Receiving Surface Data.

b. Soil-Covered Edge Data.

Figure 11. Monitoring data point line chart.

Table 1. Results of the ablation study.

C3k2-DWR	C2BRA	MFM	Focaler-CIoU	IoU (%)	MPA (%)	Params (M)
-	-	-	-	88.10	92.91	2.85
√	-	-	-	89.54	94.15	2.81
-	√	-	-	88.60	93.69	2.84
-	-	√	-	88.99	94.11	2.83
-	-	-	√	88.51	93.94	2.83
√	√	-	-	89.65	94.57	2.82
√	√	√	-	90.81	95.23	2.75
√	√	√	√	91.62	96.26	2.75

Note: A check mark (√) indicates the inclusion of the module.

Table 2. Results of the comparative experiment.

Model	mIoU (%)	MPA (%)	Recall (%)	Params (M)
Unet	83.96	90.69	83.79	2.47
DeepLabV3+	83.33	90.43	83.33	3.69
Mask-RCNN	84.51	91.52	84.96	4.11
YOLOv5n-seg	85.86	92.40	86.82	2.98
YOLOv8n-seg	86.83	92.89	87.23	2.93
YOLO11n-seg-DBM	91.62	96.26	93.10	2.75

Table 3. Monitoring system test data.

Project	Average accuracy (%)	Maximum relative error (%)	Mean relative error (%)	Maximum absolute error (cm)	Mean absolute error (cm)
Width of the light-transmitting surface of the plastic mulch	93.05	8.88	7.15	15.00	12.60
Soil coverage width at the edge of the membrane	93.02	11.11	7.35	0.60	0.44

Table 4. System alarm performance.

Project	Forward speed ($km \cdot h^{-1}$)	Average response time (s)	Alarm accuracy rate (%)	Standard deviation (s)
Plastic Film	3 km/h	1.21	95	0.060
drip tape	3 km/h	1.59	100	0.064